

⁶⁸Ga-PSMA11-PET/CT in Newly Diagnosed Carcinoma of the Prostate: Correlation of Intraprostatic PSMA Uptake with Several Clinical Parameters

Stefan A. Koerber¹⁻³ Stefan.Koerber@med.uni-heidelberg.de
Maximilian T. Utzinger⁴ m.utzinger@googlemail.com
Clemens Kratochwil^{4,5} Clemens.Kratochwil@med.uni-heidelberg.de
Claudia Kesch⁶ Claudia.Kesch@med.uni-heidelberg.de
Matthias F. Haefner¹⁻³ Matthias.Haefner@med.uni-heidelberg.de
Sonja Katayama¹⁻³ Sonja.Katayama@med.uni-heidelberg.de
Walter Mier⁴ Walter.Mier@med.uni-heidelberg.de
Andrei H. Iagaru⁷ aiagaru@stanford.edu
Klaus Herfarth¹⁻³ Klaus.Herfarth@med.uni-heidelberg.de
Uwe Haberkorn^{4,5} Uwe.Haberkorn@med.uni-heidelberg.de
Juergen Debus¹⁻³ Juergen.Debus@med.uni-heidelberg.de
Frederik L. Giesel^{4,5,8} frederik@egiesel.com *corresponding author*

1 Department of Radiation Oncology, University Hospital Heidelberg, Heidelberg, Germany

2 Clinical Cooperation Unit Radiation Oncology, German Cancer Research Center (DKFZ), Heidelberg, Germany

3 National Center of Radiation Oncology (NCRO), Heidelberg Institute of Radiation Oncology (HIRO), Heidelberg, Germany

4 Department of Nuclear Medicine, University Hospital Heidelberg, Heidelberg, Germany

5 Clinical Cooperation Unit Nuclear Medicine, German Cancer Research Center (DKFZ), Heidelberg, Germany

6 Department of Urology, University Hospital Heidelberg, Heidelberg, Germany

7 Division of Nuclear Medicine and Molecular Imaging, Stanford Health Care, Stanford, CA, USA

8 German Cancer Consortium (DKTK), Heidelberg, Germany

Corresponding author:

Frederik L. Giesel, Department of Nuclear Medicine, University Hospital Heidelberg, Im Neuenheimer Feld 400, 69120 Heidelberg, Germany; phone: +49-6221-567732; fax: +49-6221-565473; email: frederik@egiesel.com

First author:

Stefan A. Koerber, Department of Radiation Oncology, University Hospital Heidelberg, Im Neuenheimer Feld 400, 69120 Heidelberg, Germany; phone: +49-6221-5636589; fax: +49-6221-565353; email: Stefan.Koerber@med.uni-heidelberg.de

word count: 4578

Short running title: PSMA-PET/CT in primary PCa

ABSTRACT

⁶⁸Ga-prostate-specific membrane antigen (PSMA)-positron emission tomography (PET)/ computer tomography (CT) is a promising diagnostic tool for patients with prostate cancer. Our study evaluates standardized uptake values (SUV) in benign prostate tissue and malignant, intraprostatic tumor lesions and correlates results with several clinical parameters.

Methods: One hundred and four men with newly diagnosed prostate carcinoma and no previous therapy were included in this study. Maximum SUV (SUV_{max}) was measured and correlated with biopsy findings and magnetic resonance imaging (MRI). Afterwards, data was compared with current prostate specific antigen (PSA) values, Gleason score (GS) and d'Amico risk classification.

Results: In this investigation a mean SUV_{max} of 1.88 ± 0.44 in healthy prostate tissue compared to 10.77 ± 8.45 in malignant prostate lesions ($P < 0.001$) was observed. Patients with higher PSA, higher GS and higher d'Amico risk score had statistically significant higher PSMA uptake on PET/CT ($P < 0.001$ each).

Conclusion: PSMA-PET/CT is well suited for detecting the intraprostatic malignant lesion in patients with newly diagnosed prostate cancer. Our findings indicate a significant correlation of PSMA-uptake with PSA, GS and risk classification according to d'Amico scale.

Key Words: prostate cancer, PSMA-PET/CT, SUV, Gleason score, radiotherapy

INTRODUCTION

The glycosylated transmembrane protein PSMA has higher expression in prostate cancer cells compared to non-malignant prostate tissue (1,2). In the last years, several PSMA-targeting radiopharmaceuticals have been developed for diagnostic or therapeutic use in prostate cancer. One of them, Ga-68 labeled PSMA-HBED-CC (PSMA-11), showed promising results in first *in vivo* studies (3-5) and emerged as the most frequently used PSMA-targeting tracer up to date. Currently, ⁶⁸Ga-PSMA-PET/CT offers excellent diagnosis for prostate cancer in various clinical scenarios. Although modern MRI techniques like multiparametric MRI are likely to improve the detection of clinically significant cancer, there are still conflicting results e.g. concerning the role as a prebiopsy diagnostic tool (6,7). With a high sensitivity and specificity of up to 70% and 100%, PSMA-PET/CT is well suited for assessing the extent of primary prostate cancer or the detection of lymph node metastases and proved to be superior to standard routine imaging (8,9). Even compared to ¹⁸F-Choline-PET/CT, this modern diagnostic tool has high detection rates also in patients with low PSA values and negative choline imaging. (10). Although prospective, validating data is still missing, some retrospective studies reported on numerous changes in TNM stage or treatment management after ⁶⁸Ga-PSMA-PET/CT examination (11-13). One study with 57 patients performed by Sterzing et al., observed a therapy change in 50.8% of all cases (12).

There is a positive correlation between PSMA expression and GS. Several preclinical studies demonstrated that high PSMA expression was significantly correlated with higher GS (14,15). Perner et al. used tumor samples from 450 prostate cancer patients and compared PSMA expression with different clinical parameters. The authors concluded that high immunohistochemical PSMA expression in primary tumor is able to predict disease outcome independently (16). To our knowledge there is only one, larger study with robust *in vivo* data yet (17). Most of the published studies were based on tumor samples received from surgery or biopsy.

Therefore, the aim of this study is to evaluate differences of SUV measurements in healthy prostate tissue vs. malignant prostate lesions based on a high proportion of MRI/TRUS-fusion biopsy results in a large group of untreated patients with newly diagnosed prostate carcinoma undergoing PSMA-PET/CT. Besides, we perform correlations for SUV measurements and clinical parameters such as GS and d'Amico scale.

MATERIAL AND METHODS

Patient Characteristics

This study was approved by the local ethics committee (S-595/2016). Between June 2011 and February 2017 PSMA-PET/CT was performed for 177 consecutive men with newly diagnosed, treatment-naive and biopsy-proven prostate cancer in the Department of Nuclear Medicine, University Hospital Heidelberg. Forty-eight patients received androgen deprivation at the time of PSMA-PET/CT. These men were excluded from analysis due to possible effects of androgens on PSMA uptake (18-20). Because of an interval different to 60 ± 10 minutes between injection of the tracer and acquisition another 20 patients were not included in the study. We chose this interval in clinical routine for better interindividual comparability. From the remaining 109 men, sufficient clinical data was available for a total of 104 patients included in this analysis. All 104 patients underwent biopsy (48.1% multiparametric MRI/ transrectal ultrasound (TRUS)- fusion biopsy, 51.9% TRUS-guided biopsy) before imaging.

For 67 patients (64.42%), an additional multiparametric MRI scan of the prostate was performed - in the majority of cases within the preparation for biopsy. 28 men (26.92%) underwent surgery (radical prostatectomy) after PSMA-PET/CT. Only patients ($n = 42$) with additional MRI scans and histopathological data from surgery and clearly delineated, healthy tissue in the prostate were used for intraprostatic SUV comparison between normal and malignant prostate tissue to avoid incorrect measurements. For correlation with clinical parameters all patients ($n = 104$) were included except one patient with missing current PSA value.

PSMA-PET/CT Imaging

The synthesis of ^{68}Ga -PSMA-11 (median 200.5 MBq, range 92 - 338) was done as described by Eder et al. (21). 60 ± 10 minutes after intravenous injection of the tracer, PET/CT imaging was performed with a Biograph PET/CT 6 ($n = 59$) and mCT Flow ($n = 45$) scanner (Siemens, Erlangen, Germany).

A non-contrast enhanced CT scan (130 keV, 80 mAs; CareDose) was performed for attenuation correction of the PET scan. Static emission scans, corrected for dead time, scatter and decay, were acquired from the vertex to the mid-thighs, requiring eight bed positions with 3 min per bed position. The images were

reconstructed using an OSEM algorithm with 4 iterations and 8 subsets and Gaussian filtering to an in-plane spatial resolution of 5 mm at full-width at half-maximum. The CT scan was reconstructed with a B30 or B31 kernel to a slice thickness of 5 mm with an increment of 2.5 mm. For comparability of SUV values between Biograph 6 and mCT Flow we used the equivalence-SUV provided by Biograph mCT-Flow-related software syngo.

Evaluation of PSMA-PET/CT images was performed by two board certified nuclear medicine physicians and one board certified radio-oncologist by consensus. According to clinical routine at our institution, physicians were not blinded to patients characteristic. For imaging evaluation, SUV_{max} was measured in gluteal muscle, intraprostatic lesion and for patients with available MRI and pathology report in healthy prostate tissue. For calculation of the SUV_{max} of intraprostatic lesions, we drew a volume of interest around the area with the highest GS, indicated by biopsy results. A volume of interest of $10 \pm 0.15 \text{ cm}^3$ for gluteal muscle and $1 \pm 0.06 \text{ cm}^3$ for healthy prostate tissue was chosen. Healthy prostate tissue was selected in correlation with MRI and, if available, the pathology report after subsequent prostatectomy. For our analysis we chose SUV_{max} , because it offers a greater reproducibility compared to SUV_{mean} , as it doesn't depend on the size of the volume of interest (3).

Statistical Analysis

We used Microsoft Excel 2016 (*Microsoft Corporation, Redmond/ Washington, USA*) and GraphPad Prism (*Version 7.0b for Mac OS, GraphPad Software, San Diego California USA, www.graphpad.com*) for statistical analysis. Graphs were created with Sigmaplot 12 (*Systat Software Inc., San Jose California USA*). We assessed the various PSMA SUV_{max} measurements with Kruskal-Wallis-test, Mann-Whitney-test, Dunn's multiple comparisons test and Wilcoxon signed-rank test. A P value < 0.05 was considered statistically significant. To evaluate the SUV_{max} in different tissues and to generate a cut-off value to distinguish between normal intraprostatic tissue and malignant intraprostatic tissue, a receiver operating characteristic analysis was used. The provided boxplots show first and third quartile and median. The ends of the whiskers represent the 10th and the 90th percentile.

RESULTS

⁶⁸Ga-PSMA PET/CT was performed for 104 prostate cancer patients without previous local or systemic therapy. Mean SUV_{max} of gluteal muscle was 0.60 ± 0.10 for all prostate cancer patients. Healthy prostate tissue had mean SUV_{max} of 1.88 ± 0.44 compared to 10.77 ± 8.45 for malignant intraprostatic lesions in corresponding patients ($P < 0.001$; Fig. 1). Mean SUV_{max} in all 104 patients was 14.47 ± 13.87 . 46 patients (44.23%) showed unifocal uptake in the prostate. For 52 patients (50.00%) two or more loci with elevated SUV_{max} were observed, for 6 men (5.77%) the exact number of foci couldn't be determined. For 65 men (62.50%), only intraprostatic tracer uptake was detected. 32.69% ($n = 34$) of prostate cancer patients undergoing PSMA-PET/CT were diagnosed with lymphatic metastases, 18.27% ($n = 19$) with bone metastases and 11.54% ($n = 12$) with bone and lymphatic metastases (in total 38 bone metastases in 19 patients). Lymph node metastases were located within the pelvis for 17 patients (16.35%; Table 1). One patient with lung metastases and one patient with a penile metastasis were diagnosed. Comparing PSMA-PET/CT with available MRI data, there was a match of detection of intraprostatic tumor lesions with highest available GS in 89.55%.

After correlation of intraprostatic, tumor-related tracer uptake with clinical parameters, a mean SUV_{max} of 8.55 ± 5.88 was detected in patients with current PSA values of < 10 ng/ml compared to 14.97 ± 16.20 for PSA values of 10-20 ng/ml and 19.47 ± 15.47 for PSA values of more than 20 ng/ml ($P < 0.001$). Correlating SUV_{max} and GS, prostate cancer lesions from biopsy with GS 6 and 7 had mean SUV_{max} of 6.74 ± 6.10 and 11.06 ± 11.56 , respectively (Fig. 2). The highest tracer uptake was found in intraprostatic lesions with GS of 9, with a mean SUV_{max} of 22.16 ± 18.46 . Prostate cancers with high GS (8 – 10) showed a statistically significant higher PSMA uptake (mean SUV_{max} of 19.61 ± 15.44) than tumors with a GS of 6 or 7 (mean SUV_{max} of 9.88 ± 10.49 ; $P < 0.001$). In ungrouped analyses, differences remained statistically significant for GS 6 – 10 as well as for grading system according to International Society of Urological Pathologists ($P < 0.001$ each; Fig. 3). Significant differences were also observed for risk classification based on the d'Amico scale (22): patients with high risk tumors had higher intraprostatic PSMA uptake (mean SUV_{max} of 16.67 ± 14.88) compared to tumors with low (mean SUV_{max} of 5.97 ± 3.69) and intermediate risk (mean SUV_{max} of 6.98 ± 4.11) ($P < 0.001$; Table 2).

For subgroup analysis, correlations of intraprostatic SUV_{max} with clinical parameters were performed considering histopathological data from surgery and biopsy type (MRI/TRUS-fusion biopsy). Comparison of clinical parameters with histological results only obtained from MRI/TRUS-fusion biopsy also revealed statistically significant higher uptake in tumors with GS 8-10 than in those with GS 6-7 (mean SUV_{max} 11.24 ± 12.9 and 19.45 ± 17.24 , $P = 0.004$). From 28 men undergoing prostatectomy mean SUV_{max} was 14.10 ± 11.07 ($n = 15$) for GS 7 tumors, compared to 20.41 ± 11.51 ($n = 13$) for GS 8-10 tumors (Fig. 4). This difference of intraprostatic tracer uptake was only of borderline significance ($P = 0.142$; Table 3). The correlation of histopathological results from surgery with malignant, intraprostatic lesions obtained from ^{68}Ga PSMA-PET/CT leads to a calculated PET-sensitivity and specificity of 68 and 92%. For PET/CT data correlating with MRI, there was a total or near-total match of increased tracer uptake in the same prostate segments in 91%.

DISCUSSION

To our knowledge, this is the largest study evaluating the role of ^{68}Ga PSMA-PET/CT as a primary staging tool for intraprostatic tumor lesions and the correlation with clinical and prognostic factors. Together with MRI and post-surgery histopathological data as a reference test, we observed a statistically significant difference in mean SUV_{max} measurements between benign and malignant prostate tissue ($P < 0.001$). Intraprostatic lesions in 42 patients suspected for malignancy showed mean SUV_{max} of 10.77 ± 8.45 which is comparable to other findings. The average SUV_{max} of histopathology-positive segments was 11.8 ± 7.6 in a recently published study of 21 patients with biopsy-proven prostate cancer (23). Fendler et al. reported on a mean SUV_{max} of 4.9 ± 2.9 for non-diseased segments (23) in comparison with 1.88 ± 0.44 in our study. Although a small cohort, a statistically significant difference was also observed for intraprostatic prostate cancer lesions and non-prostate cancer tissue in a group of nine patients with histopathological proven primary carcinoma of the prostate who underwent ^{68}Ga -PSMA-PET/CT followed by radical prostatectomy (24). In receiver operating characteristic analyses (data not shown) a SUV_{max} cut-off of > 2.73 would lead to a sensitivity and specificity of 100% and 97.62% (95% confidence interval 91.59% to 100% and 87.43% to 99.94%) in our cohort, respectively. These results need to be treated with caution due to the relatively small number of cases with histopathological

information and the arguable SUV measurements based on multiparametric MRI. Nevertheless, PSMA-PET/CT seems to be a promising, diagnostic tool for the identification of malignant segments in the prostate. These findings are in accordance with results from 30 high-risk prostate cancer patients undergoing PSMA-PET/CT imaging prior to radical prostatectomy. Budäus et al. reported, that in 92.9% of patients, the intraprostatic tumor foci were predicted correctly (25). Therefore, PSMA-PET/CT may play an important role not only in detecting metastases, but also for localization of tumor segments in the prostate. Similar to MRI-supported biopsy, cancer lesions can be traced with reference to PET imaging to avoid false-negative results or understaging of the tumor regarding the detection of the highest Gleason pattern. There might be a high potential to improve the current standard TRUS-biopsy in the same way as MRI did. Lower rates of indolent cancer detection and a bigger proportion of identification of intermediate and high-risk tumors using MRI/TRUS-fusion biopsy have already been described (26). Further studies are needed to evaluate the role of ^{68}Ga PSMA-PET/CT for prostate biopsy, also with regard to cost efficiency.

Furthermore, we investigated the correlation of intraprostatic PSMA uptake and several clinical parameters in subgroup analysis. Among a statistically significant difference of SUV_{max} regarding the present PSA, we also observed a significantly higher mean SUV_{max} in tumors with higher d'Amico risk classification and GS from biopsy ($P < 0.001$ for grouped analyses). In consideration of a small number of patients, these differences remained statistically significant ($P < 0.001$ each) in ungrouped evaluation (Fig. 5). There seems to be a strong trend of rising PSMA uptake with higher grade malignancy. To our knowledge, there is only one larger, recently published study apart from research using tissue microarrays which also described a correlation of tracer accumulation and clinical parameters: Uprimny et al. observed significantly lower PSMA uptake in tumors with GS 6 – 7b and $\text{PSA} < 10$ ng/ml in a cohort of 90 men. The median SUV_{max} of intraprostatic, malignant lesions was 11.5 ng/ml compared to 3.9 ng/ml in normal prostate tissue (17). This relatively high SUV_{max} in healthy prostate tissue could be related to the fact, that for calculation of SUV_{max} the tumor site was only verified by TRUS-guided biopsy, which has been proven insufficient (27). In contrast MRI/TRUS-fusion biopsy comprising targeted and systematic cores– which was done for nearly 50% of the patients in our cohort - leads to a precise definition of malignant and non-malignant areas in the prostate (28). It is interesting to note, that Uprimny et al. observed a lower SUV_{max} in GS 10 (17.7) tumors compared to GS 9 (22.8) (17) - in the same

way as we did (GS 10: 18.3; GS 9: 22.2) – assuming that lower, intraprostatic tracer uptake is caused by dedifferentiation of tumor cells in GS 10 prostate carcinomas.

Another analysis performed by Fendler et al. observed a significantly lower SUV_{max} in histopathology-positive segments with GS of 6 compared to segments with GS of 7 or more with a P value of 0.012. However, no statistically significant difference was reported for segments with a GS of 7 or more (23). The relatively small-sized cohort ($n = 21$) and the small number of patients with a high GS (GS 8: 3 men; GS 9: 7 men) might explain the lack of difference compared to our findings.

Especially for definitive radiotherapy, identification of high malignant intraprostatic cancer segments is extremely helpful, because of the high risk for local recurrence of these so called “dominant intraprostatic tumor lesions” after local treatment (29,30). The concept of treating dominant intraprostatic tumor lesions with an increased dose (boost) to improve local control is objective of a currently recruiting randomized phase III trial (FLAME-trial) that is, however, based on MRI-guided definition of dominant intraprostatic tumor lesions (31). It has recently been shown, that delineation of target volume and dominant intraprostatic tumor lesions is also feasible with PSMA-PET/CT (32). Due to some benefits of PET scan compared to MRI scans, irradiation planning based on PSMA-PET/CT would be of great interest (Fig. 6).

The major limitations of our study are its retrospective nature and the small number of histopathological results from prostatectomy. Most patients underwent radiotherapy or androgen deprivation after PSMA-PET/CT, why validated, histopathological data from surgery is only available for 26.92%. Besides, for clinical correlation (e.g. high GS) only a few patients could be included in our analyses. On the other hand, our study is one of the largest evaluating the role of PSMA-PET/CT for intraprostatic tumor detection and correlation of SUV_{max} with Gleason score and risk classification. Hence, our data can be used as a basis for further, prospective studies.

CONCLUSION

Our study confirms that PSMA-PET/CT is an excellent diagnostic tool for the detection of intraprostatic tumor lesions. As one of the first analyses in a large patient cohort our results indicate a correlation of tracer

uptake with GS and d'Amico risk classification. This information might be very useful for further diagnostic procedures i.e. biopsy-guidance and treatment planning in radiation oncology.

DECLARATION

List of Abbreviations

CT	computer tomography
GS	Gleason score
MRI	magnetic resonance imaging
PET	positron emission tomography
PSA	prostate specific antigen
PSMA	prostate specific membrane antigen
SUV	standardized uptake value
TRUS	transrectal ultrasound

Financial Disclosure

All authors had no relevant financial relationship to disclose.

Competing Interests

The authors indicated no potential conflicts of interest.

Acknowledgments

The authors express their sincere gratitude to Tim Holland-Letz for his excellent statistical assistance.

This research was supported in part by the Klaus-Tschira-Stiftung (project no. 00.198.2012).

REFERENCES

1. Silver DA, Pellicer I, Fair WR, Heston WD, Cordon-Cardo C. Prostate-specific membrane antigen expression in normal and malignant human tissues. *Clin Cancer Res.* 1997;3:81-85.
2. Bostwick DG, Pacelli A, Blute M, Roche P, Murphy GP. Prostate specific membrane antigen expression in prostatic intraepithelial neoplasia and adenocarcinoma: a study of 184 cases. *Cancer.* 1998;82:2256-2261.
3. Afshar-Oromieh A, Malcher A, Eder M, et al. PET imaging with a [68Ga]gallium-labelled PSMA ligand for the diagnosis of prostate cancer: biodistribution in humans and first evaluation of tumour lesions. *Eur J Nucl Med Mol Imaging.* 2013;40:486-495.
4. Afshar-Oromieh A, Zechmann CM, Malcher A, et al. Comparison of PET imaging with a (68)Ga-labelled PSMA ligand and (18)F-choline-based PET/CT for the diagnosis of recurrent prostate cancer. *Eur J Nucl Med Mol Imaging.* 2014;41:11-20.
5. Dietlein M, Kobe C, Kuhnert G, et al. Comparison of [(18)F]DCFPyL and [(68)Ga]Ga-PSMA-HBED-CC for PSMA-PET imaging in patients with relapsed prostate cancer. *Mol Imaging Biol.* 2015;17:575-584.
6. Ahmed HU, El-Shater Bosaily A, Brown LC, et al. Diagnostic accuracy of multi-parametric MRI and TRUS biopsy in prostate cancer (PROMIS): a paired validating confirmatory study. *Lancet.* January 19, 2017 [Epub ahead of print].
7. Tonttila PP, Lantto J, Pääkkö E, et al. Prebiopsy multiparametric magnetic resonance imaging for prostate cancer diagnosis in biopsy-naive men with suspected prostate cancer based on elevated prostate-specific antigen values: results from a randomized prospective blinded controlled trial. *Eur Urol.* 2016;69:419-425.
8. Maurer T, Gschwend JE, Rauscher I, et al. Diagnostic efficacy of (68)Gallium-PSMA positron emission tomography compared to conventional imaging for lymph node staging of 130 consecutive patients with intermediate to high risk prostate cancer. *J Urol.* 2016;195:1436-1443.

9. Giesel FL, Sterzing F, Schlemmer HP, et al. Intra-individual comparison of (68)Ga-PSMA-11-PET/CT and multi-parametric MR for imaging of primary prostate cancer. *Eur J Nucl Med Mol Imaging*. 2016;43:1400-1406.
10. Bluemel C, Krebs M, Polat B, et al. 68Ga-PSMA-PET/CT in patients with biochemical prostate cancer recurrence and negative 18F-choline-PET/CT. *Clin Nucl Med*. 2016;41:515-521.
11. Shakespeare TP. Effect of prostate-specific membrane antigen positron emission tomography on the decision-making of radiation oncologists. *Radiat Oncol*. 2015;10:233.
12. Sterzing F, Kratochwil C, Fiedler H, et al. (68)Ga-PSMA-11 PET/CT: a new technique with high potential for the radiotherapeutic management of prostate cancer patients. *Eur J Nucl Med Mol Imaging*. 2016;43:34-41.
13. Dewes S, Schiller K, Sauter K, et al. Integration of (68)Ga-PSMA-PET imaging in planning of primary definitive radiotherapy in prostate cancer: a retrospective study. *Radiat Oncol*. 2016;11:73.
14. Minner S, Wittmer C, Graefen M, et al. High level PSMA expression is associated with early PSA recurrence in surgically treated prostate cancer. *Prostate*. 2011;71:281-288.
15. Kasperzyk JL, Finn SP, Flavin R, et al. Prostate-specific membrane antigen protein expression in tumor tissue and risk of lethal prostate cancer. *Cancer Epidemiol Biomarkers Prev*. 2013;22:2354-2363.
16. Perner S, Hofer MD, Kim R, et al. Prostate-specific membrane antigen expression as a predictor of prostate cancer progression. *Hum Pathol*. 2007;38:696-701.
17. Uprimny C, Kroiss AS, Decristoforo C, et al. 68Ga-PSMA-11 PET/CT in primary staging of prostate cancer: PSA and Gleason score predict the intensity of tracer accumulation in the primary tumour. *Eur J Nucl Med Mol Imaging*. January 31, 2017 [Epub ahead of print].
18. Hope TA, Truillet C, Ehman EC, et al. 68Ga-PSMA-11 PET imaging of response to androgen receptor inhibition: first human experience. *J Nucl Med*. 2017;58:81-84.
19. Meller B, Bremmer F, Sahlmann CO, et al. Alterations in androgen deprivation enhanced prostate-specific membrane antigen (PSMA) expression in prostate cancer cells as a target for diagnostics and therapy. *EJNMMI Res*. 2015;5:66.

20. Wright GL, Jr., Grob BM, Haley C, et al. Upregulation of prostate-specific membrane antigen after androgen-deprivation therapy. *Urology*. 1996;48:326-334.
21. Eder M, Schäfer M, Bauder-Wüst U, et al. ⁶⁸Ga-complex lipophilicity and the targeting property of a urea-based PSMA inhibitor for PET imaging. *Bioconjug Chem*. 2012;23:688-697.
22. D'Amico AV, Whittington R, Malkowicz SB, et al. Biochemical outcome after radical prostatectomy, external beam radiation therapy, or interstitial radiation therapy for clinically localized prostate cancer. *JAMA*. 1998;280:969-974.
23. Fendler WP, Schmidt DF, Wenter V, et al. ⁶⁸Ga-PSMA PET/CT detects the location and extent of primary prostate cancer. *J Nucl Med*. 2016;57:1720-1725.
24. Zamboglou C, Schiller F, Fechter T, et al. (⁶⁸Ga)HBED-CC-PSMA PET/CT versus histopathology in primary localized prostate cancer: a voxel-wise comparison. *Theranostics*. 2016;6:1619-1628.
25. Budäus L, Leyh-Bannurah SR, Salomon G, et al. Initial experience of (⁶⁸Ga)PSMA PET/CT imaging in high-risk prostate cancer patients prior to radical prostatectomy. *Eur Urol*. 2016;69:393-396.
26. Siddiqui MM, Rais-Bahrami S, Turkbey B, et al. Comparison of MR/ultrasound fusion-guided biopsy with ultrasound-guided biopsy for the diagnosis of prostate cancer. *JAMA*. 2015;313:390-397.
27. Ahmed HU, El-Shater Bosaily A, Brown LC, et al. Diagnostic accuracy of multi-parametric MRI and TRUS biopsy in prostate cancer (PROMIS): a paired validating confirmatory study. *Lancet*. 2017;389:815-822.
28. Radtke JP, Schwab C, Wolf MB, et al. Multiparametric magnetic resonance imaging (MRI) and MRI-transrectal ultrasound fusion biopsy for index tumor detection: correlation with radical prostatectomy specimen. *Eur Urol*. 2016;70:846-853.
29. Arrayeh E, Westphalen AC, Kurhanewicz J, et al. Does local recurrence of prostate cancer after radiation therapy occur at the site of primary tumor? Results of a longitudinal MRI and MRSI study. *Int J Radiat Oncol Biol Phys*. 2012;82:787-793.
30. Bott SR, Ahmed HU, Hindley RG, Abdul-Rahman A, Freeman A, Emberton M. The index lesion and focal therapy: an analysis of the pathological characteristics of prostate cancer. *BJU Int*. 2010;106:1607-1611.

31. Lips IM, van der Heide UA, Haustermans K, et al. Single blind randomized phase III trial to investigate the benefit of a focal lesion ablative microboost in prostate cancer (FLAME-trial): study protocol for a randomized controlled trial. *Trials*. 2011;12:255.
32. Zamboglou C, Wieser G, Hennies S, et al. MRI versus ^{68}Ga -PSMA PET/CT for gross tumour volume delineation in radiation treatment planning of primary prostate cancer. *Eur J Nucl Med Mol Imaging*. 2016;43:889-897.

FIGURES

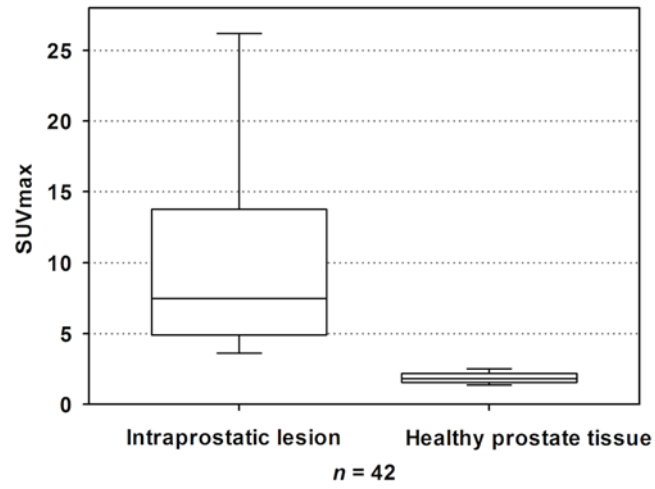


FIGURE 1: Boxplot of SUV_{max} from malignant (*left*) and normal (*right*) intraprostatic tissue

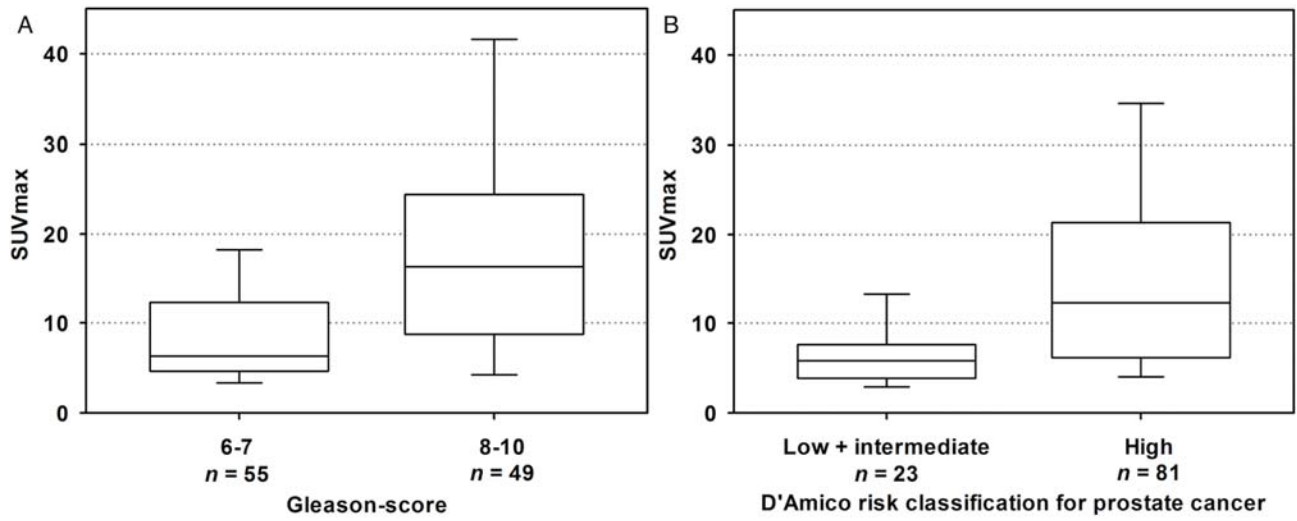


FIGURE 2: Boxplot of SUV_{max} according to Gleason score in biopsy (A) and d'Amico classification (B)

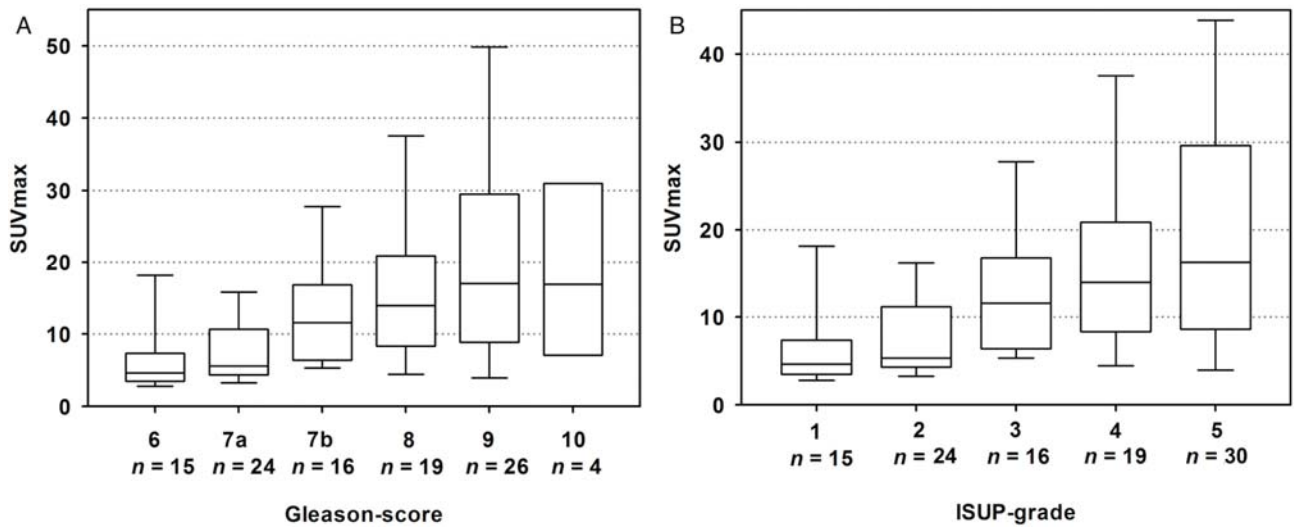


FIGURE 3: Boxplot of SUV_{max} according to ungrouped Gleason score in biopsy (A) and to International Society of Urologic Pathologists (ISUP) -grade in biopsy (B)

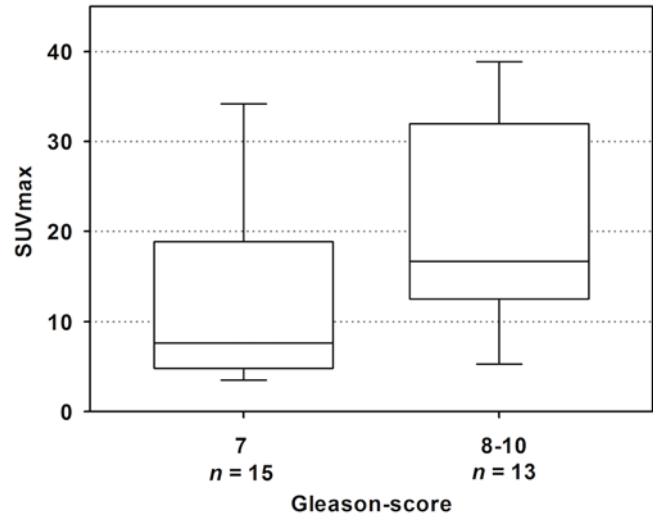


FIGURE 4: Boxplot SUV_{max} of GS (grouped) after prostatectomy

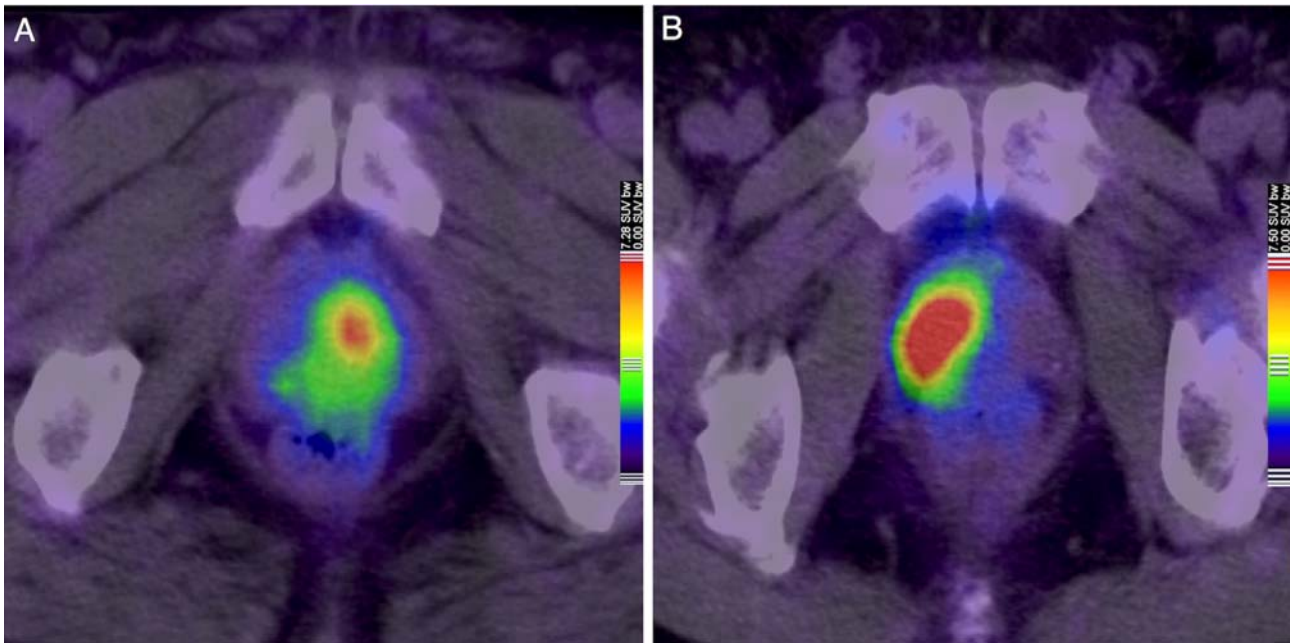


FIGURE 5: Different PSMA tracer uptake according to Gleason score: one patient with GS 6 prostate cancer and SUV_{max} of 7.33 (A) compared to a GS 9 tumor and SUV_{max} of 16.64 (B)

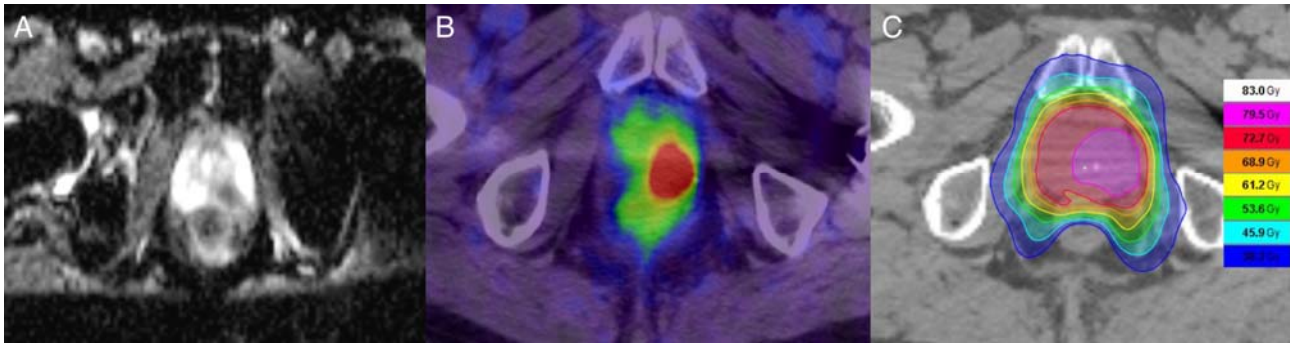


FIGURE 6: Relevant data for an intraprostatic boost during radiotherapy: MRI of the prostate with ADC-sequence (A), PSMA tracer uptake in PSMA-PET/CT (B) and radiation plan with irradiation of the prostate and simultaneous integrated boost according to pretreatment imaging (C)

TABLES

TABLE 1: Patient's characteristics

	all patients (n = 104)		all patients (n = 104)
median age [years]	67.4 (range 38 - 84)	Gleason score (biopsy)	
clinical tumor stage		6	15
T1a	-	7a	24
T1b	-	7b	16
T1c	39	8	19
T2a	1	9	26
T2b	1	10	4
T2c	25	current PSA	
T3a	7	< 10 ng/ml	35
T3b	26	10 – 20 ng/ml	30
T4	5	> 20 ng/ml	38
N0	72	unknown	1
N1	32	d'Amico score (21)	
M0	82	low risk	6
M1a	3	intermediate risk	17
M1b	17	high risk	81
M1c	2		

TABLE 2: Comparison of SUV_{max} and clinical parameters

Clinical parameters	median	mean SUV _{max}	standard deviation	<i>P</i> -value
current PSA (n = 103)				
< 10	5.98	8.55	5.88	< 0.001
10 – 20	7.94	14.97	16.20	
> 20	14.77	19.47	15.47	
Gleason score in biopsy (grouped; n = 104)				
6-7	6.28	9.88	10.49	< 0.001
8-10	16.29	19.61	15.44	
Gleason score in biopsy (n = 104)				
6	4.62	6.74	6.10	< 0.001
7a	5.56	9.74	13.47	
7b	11.56	13.04	7.89	
8	13.94	16.4	10.75	
9	16.99	22.16	18.46	
10	16.88	18.30	12.45	
d'Amico score (grouped; n = 104)				
low/intermediate risk	5.79	6.72	3.95	< 0.001
high risk	12.27	16.67	14.88	
d'Amico score (n = 104)				
low risk	5.12	5.97	3.69	< 0.001
intermediate risk	5.79	6.98	4.11	
high risk	12.27	16.67	14.88	

TABLE 3: Comparison of SUV_{max} and GS in MR guided biopsy and prostatectomy

Gleason score in MR guided biopsy (grouped; n = 50)	median	mean SUV_{max}	standard deviation	<i>P</i>-value
7	7.59	11.24	12.9	0.004
8-10	13.12	19.45	17.24	
Gleason score after prostatectomy (grouped; n = 28)				
7	8.32	14.1	11.07	0.14
8-10	16.64	20.41	11.51	